第 15 卷 第 3 期
1997 年 9 月

天 文 学 进 展
PROGRESS IN ASTRONOMY

Vol.15, No.3
Sep., 1997

太阳大气磁精细结构的射电探讨

傅 其 骏

(中国科学院北京天文台 北京 100080)

摘 要

太阳大气磁场的研究对于太阳大气物理及太阳活动研究是十分重要的。目前探测光球以外的日冕、色球、过渡区磁场的几乎唯一办法，是在紧密联系其他频谱段取得的信息基础上使用射电观测。根据在微波、米波段有关辐射机制和传播过程，介绍了推导磁场讯息的基本射电方法。在按高度分布的磁场上，还存在磁场的精细结构，这被认为是与裂化的场耗散(重连)紧密相关，并产生以射电辐射显现出来的粒子加速及等离子体加热。微波爆发中快速精细结构的动态频谱为精细磁结构的诊断提供了一种重要的手段，这也是我国正在建立中的作为太阳活动第 23 周极大期重点项目的“太阳射电宽带频谱仪”的主要科学目标。

关 键 词 太阳：日冕 — 太阳：磁场 — 太阳：耀斑 — 太阳：色球 — 辐射机制：热 — 辐射机制：非热

The Radio Approach of Magnetic Fine Structures in Solar Atmosphere

Fu Qijun

(*Beijing Astronomical Observatory, The Chinese Academy of Sciences, Beijing* 100080)

Abstract

(*Received 1996 May 7*)

The investigation on the magnetic field in solar atmosphere is essential not only to solar atmosphere physics but also to solar activity. Radio observation in close connection with information obtained in other spectral range, e.g. the optical and X-ray regions is almost a unique method for the determination of magnetic field in the coronal and chromosphere outside the photomosphere. On the base of relevant mechanism of emission and propagation processes in microwave and meter wavebands, basic radio methods for the deduction of the information

1996 年 5 月 7 日收到

on magnetic fields of background and source region are introduced. There is evidence for the existence of fine structures superimposed on the mean background height distribution of magnetic fields, which are expected to be intimately related to fragmentary field dissipation (reconnection) leading to particle acceleration and plasma heating signified by radio emission. The radio dynamic spectra of fast fine structures (FS) in microwave bursts provide a significant means for the diagnosis of fine magnetic structures. It is also the major scientific objects of "Solar Radio Broadband Spectrometer" which is being set up as a key project for the 23rd solar activity cycle.

Key words Sun: radio radiation—Sun: magnetic fields—Sun: corona—Sun: flares—Sun: chromosphere—radiation mechanism: thermal—radiation mechnism: non-thermal

1 Introduction

The existence of the magnetic field and magnetic activity is the cause and energy sources of almost all of the active phenomena in the Sun and Sun-like stars. Were it not the case for its magnetic field the Sun might well be a uniform sphere of gas entirely devoid of interesting, changing structures, such as sunspots, prominences, flares and mass ejection, and radiation might be undetectable in X-rays and radio waves[1].

Kruger and Hildebrandt[2] pointed out that major problems of the physics of the solar atmosphere and processes of solar activity are due to the poor knowledge of the magnetic fields outside the photosphere. Although qualitative evidence for magnetic field in the chromoshpere and corona can be found in observations in different spectral regions from X-rays to optical waves, radio waves are favored to produce quantitative information on magnetic field.

One can observe the inner corona in the three main spectral regions, optical, radio and shortwaves (EUV, X-rays), each of them having its own domain of information. The main limitation for the optical observations is that the corona can be seen only outside the solar disk, and the limits for EUV and X-rays observations are mostly connected with high expenses needed for observations from space and only episodic series of observations can be obtained. The radio observations in principle can overcome the above limitations for the other methods.

The radio methods, however, in contrast to Zeeman effect of optical waves in the photosphere, mostly concern indirect methods of the determination of magnetic fields and typically require additional information or working hypotheses, based on the reasonably assuming of the mechanisms of radiation and propagation process. Due to the fact that the radio emission in different wavebands is from different layers of solar atmosphere, the magnetic intensity and other magnetic information at different layers of solar atmosphere can be deduced by making observations in different wavebands (millimeter, centimeter, decimeter and meter wavelengths).

The basic principle for radio methods to measure the solar magnetic field is different from the Zeeman effect for optical methods . The coronal thermal plasma, due to the presence of magnetic field, becomes non-homogeneous, and the propagating electromagnetic wave will be

split into ordinary and extraordinary modes. Under the conditions in solar atmosphere, the circular polarization (left circular polarization–LCP, or right circular polarization–RCP), which reflect the differences between the two modes, are measured. The LCP (or RCP) associated with N pole, while the RCP (or LCP) associates with S pole. It is valuable only if the polarization observations are with high spatial resolution, because the sunspots appear on solar disk in pairs and the global polarization degree of full solar disk is close to zero . In the early stage of solar radio astronomy, solar eclipse provides a good opportunity to make one dimension polarization observation. The circular polarization from following spots appears as soon as the leading spots with reverse polarity are occulted by the Moon's limb. In the case of radio bursts which have small source regions, in particular of millisecond burst sources with a spatial scale of only tens to 200 km (0″.05—0″.3), radio observation can obtain fine magnetic field information in source regions. Some detailed description can be found in the following sections.

Gelfreikh[3,4] summarized that polarization observation made with a high spatial resolution and high spectral resolution instrument is capable of measuring the magnetic field in the solar corona. Three methods have been developed using the RATAN-600 observation, based on different mechanisms of radiation and propagation of radio wave in the solar atmosphere. Using the RATAN-600 with the new Panoramic Analyzer of the Spectrum (PAS), this new technique produces a measurement accuracy of $\sim 3\%$ for magnetic fields of sunspots at the base of the solar corona, with the "radio" magnetic fields being weaker than the "optical" by $\approx 20\%$.

Lang *et al.*[5] synthesized the detailed spectral polarization observations of the RATAN-600 in 1.7–32cm waveband and the high spatial resolution observations of the VLA at 2.0, 3.5, 6.2 and 20.7cm wavelengths, which have been used to infer the physical parameters of a number of quiescent active region structures, using the theory of cyclotron emission to show that the magnetic field strength in the corona above large sunspots is often 75%–80% of the magnetic field strength in the underlying sunspots. Being comparing with those obtained from potential field extrapolations, the results suggest that the coronal fields diverge more slowly than expected for a dipole located below the solar surface. Using five-element array of Owens Valley Observatory of Caltech, Lee, Gary and Hurford[6] have obtained some similar results. Some results of the magnetic field of microwave burst source regions have also been obtained with high spatial resolution imaging radio telescope, such as VLA.

In the research on rapid radio fluctuation in solar flares, the findings of millisecond FS in microwave bursts provide significant and promising approach for the probing of magneto-plasma fine structures in solar atmosphere. In general, the radio burst emission is the manifestation of the interaction of the energetic particles (electrons) produced in flares on ambient plasma and magnetic fields. The radio bursts with different time scales are the manifestation of energy release processes with different time scales, which should relate to some specific electron distribution and magnetic configuration. Consequently, the study of microwave bursts with different time scale, in particular of their dynamic radio spectra should be able to find the important information about small fine structures of the magnetic fields. It is also one of major objects of "Solar Radio

Broadband Spectrometer" which is being set up as a key project for the 23rd solar activity cycle. So, it is an important field of research for Chinese solar radio astronomers during the coming solar active maximum period.

2 The radio measurements of the coronal magnetic field

As introduced in [2], [3], [4] and [5], the radio polarization observation with high spatial resolution and high spectral resolution is capable of measuring magnetic fields in the solar corona. Based on the different mechanisms of radiation and propagation processes of radio wave in solar atmosphere, there are three methods, namely, thermal bremsstrahlung, thermal cyclotron emission, and inversion of polarization in QT-region (quasi-transverse-region).

2.1 Thermal bremsstrahlung[3]

For the thermal plasma emission in the presence of magnetic field the radiation is generally circularly polarized due to the difference of the opacity for ordinary and extraordinary modes of magneto-ionic theory. For the case of not very strong magnetic field ($f_B \ll f$, f_B–magnetic gyrofrequency, f-frequency of observations) , the solution of the transfer-equation may be written for degree of polarization[8]:

$$P = n(f_B/f)\cos\alpha, \tag{1}$$

where α is angle of direction of magnetic field, $n = -\mathrm{d}(\ln T_B)/\mathrm{d}(\ln f)$ the spectral index, and T_B is brightness temperature. We can get the longitude component of the magnetic field B_l as

$$B_l = 107 \cdot P(\%)/(n \cdot \lambda), \tag{2}$$

where λ is the wavelength of observations.

This method has been used to measure magnetic field in coronal loops and flocculi. It has been shown that at the base of the corona in a flocculus the magnetic field intensity is practically the same as at the photospheric level, while at the top of a loop it was found to be (about 20G at the height about 7×10^4km) of the order expected from simple potential extrapolation of photospheric fields.

2.2 Thermal cyclotron emission[4]

The solar slow variation component emission associated with active regions in centimeter and decimeter wavebands can be interpreted with low harmonic gyroresonant radiation ($s \leq 4$) of thermal electrons of the corona, so it can be used to measure the magnetic field of solar active regions. Some authors[9–12] have presented useful models. This method can also be used for some coronal loops in decimeter wavelength range and some "radiogranules". The magnetic field strength and observing wavelength λ are connected in the following way:

$$\begin{aligned} B_t &= 5400/\lambda \quad \text{(for the second harmonic)}, \\ B_t &= 3570/\lambda \quad \text{(for the third harmonic)}. \end{aligned} \tag{3}$$

We may often distinguish the second and third harmonic using polarization measurements (the third harmonic is strongly circularly polarized). Spectral observations (spectral resolution of $0.1f$)

show that for each sunspot associated with radio source one can find the shortest wavelength, λ_c critical wavelength (mostly in the range from 2 to 3cm, for large sunspot, the λ_c is shorter) generated by this mechanism . Substituting λ_c for λ in the formula (3) for the third harmonic, the magnetic field strength above sunspots in the corona can be obtained. Analysis made for a large number of sunspots has shown that radio magnetic fields are in good correlation with optical ones measured from Zeeman splitting at photospheric level. The former are generally only $\approx 20\%$ lower than the relevant strongest magnetic fields at the photospheric level and often exceed such a high value as 2000G. In some cases it has been found that coronal magnetic field could change (increase) without changes of the photosphere field of the same sunspots. This process precedes the development of an old active region and so may be a prognostic.

It is found that the results of the magnetic field measurements of the same sunspot made in the chromosphere–coronal transition region (CCTR) using UV carbon (CIV) line from the SMM satellite are in contradiction with those from radio observations made with the RATAN -600. The problem is that the radio fields prove to be significantly (by a factor of about 1.5) higher than UV values. A possible solution of this contradiction is an extremely inhomogeneous model of the CCTR above a sunspot. But the whole problem is certainly worth making efforts for further observational data and more well-based and elaborate models.

2.3 Wave propagation effects-inversion of polarization in QT-region[3]

A number of wave propagation effects can be applied to the diagnostics of coronal magnetic field, e.g. the reversal of polarization in a region of quasi-transverse propagation (QT-region) and Faraday effect. When an electromagnetic wave crosses the region of quasi-transverse magnetic field with the inversion of direction of the longitude magnetic field, the sign of circular polarization of the wave may invert[13]. The effect depends on the wave frequency and parameters of the QT-region. From the formula of the critical frequency at which the sign of circular polarization inverts, a simple formula for measuring magnetic field in QT-region in the solar corona may be obtained, i.e.,[14]

$$B_i = 1.57 \times 10^8 / \lambda (\lambda_i N_e L_B)^{1/3}, \tag{4}$$

or roughly

$$B_i \doteq 43/\lambda_i, \tag{5}$$

where λ_i is the wavelength (cm) of the inversion of polarization, N_e the electron density, and L_B the scale length of the magnetic field.

The use of this method for a number of active regions has shown that the distribution of the magnetic fields in the corona is in general in agreement with the ones extrapolated from the photosphere level in potential approximation. That is generally true for the heights from 20 to 100 thousand km. Important local deviations are met , however, especially in flaring active regions. The value of 10 to 40 G seems to be typical for the heights of 70 to 120 thousand km above the photosphere.

2.4 Gyro-synchrotron radiation

In literature [2], it has also been pointed out that gyromagnetic radiation at higher harmonics corresponding to greater energy of the emitting electrons (called gyro-synchrotron radiation) has been applied to radio burst emission, and the information about the magnetic field can be extracted from the shape (frequency extent) and position (spectral maximum) of the emitted spectrum. Thus, the magnetic fields in source regions of radio bursts can be obtained.

From the theoretical point of view, microwave spectroscopy should have the potentiality to diagnose the behavior of energetic electrons and magnetic field in a burst source, but additional assumptions are usually necessary to separate the properties of magnetic fields from those of the electron distribution. It seems to be impossible to calculate the magnetic field from the complicated relation of the gyro-synchrotron radiation or synchrotron radiation before the simplified expressions of the two type of radiations were given by Dulk, Marsh[15] and Dulk[16]. After that, using some assumptions some authors[17−19] presented the estimative formulas of magnetic fields in burst source regions. Zhou and Karlicky[20], and Zhou[21] decreased the number of these assumptions, with T_b (the source brightness temperature) only, and presented a more direct useful way to calculate the magnetic field in microwave source. The formula is as follows,

$$B = \left(c^2/(kT_bA_1)\nu_{peak}^{1.30+0.98\delta}\nu^{-0.78-0.90\delta}A_2^{-2.52-0.08\delta}\right)^{\frac{1}{0.52+0.08\delta}}, \tag{6}$$

where $A_1 = 4.24\times10^{14}10^{0.3\delta}(\sin\theta)^{0.34+0.07\delta}$, $A_2 = 2.8\times10^6$, δ-the power-law energy index of electrons,θ-the viewing angle, k-Boltzmann constant, ν_{peak}-the peak frequency of intensity spectrum at maximum time. Therefore the term NL, which is the total number of superthermal electrons along the line of sight, can be obtained. Consequently, the solar radio broadband spectrometer, which is being set up, will play an important role in the aspect of the magnetic field measurement in microwave burst source regions.

3 Temporal fine structures in microwave bursts and magnetic microstructures in corona

3.1 The time profiles with different time scale of microwave bursts

The time profiles of radio bursts are the morphological features which have been studied for long time and analyzed most extensively. Time scale is one of the important characteristics of time profiles of radio bursts. The duration of bursts are from fractions of second to hours. According to time profiles, radio bursts can be morphologically classified in simple impulsive type, gradual rise and fall type and complicated type. In comparing with the radio bursts in metric wavelength, the microwave bursts are more smooth and details-less. But in some microwave bursts, there appear complicated pulses and pulse groups with different time scales superimposed on the slow varying burst background. A microwave burst with complicated time profile and different types of time structures, recorded by Beijing Astronomical Observatory (BAO) at 2840MHz frequency is illustrated as a typical example in Figure 1[22], in which the main part of the burst consists of numerous steps with much steeper flux rising than the envelope subpulses may recur at a quasi-

periodic repetition rate, flux pulsations may occur, and subsecond and shorter time duration spike are found to be superposed on a slowly varying emission. From this one can distinguish a sequence of different time scales in five ranges:

(1) tens minute duration of the main burst;

(2) a few minute duration of the main burst pulses;

(3) a few second duration of the pulses, which are a prominent feature of hard X-ray records (elementary bursts), and the time scale of type III burst groups;

(4) a few fractions of second duration of the subpulses, which are a prominent feature of mm-wave burst records (sub-bursts), and the time scale of single type III burst; and

(5) shorter than 0.1 second duration of fine structures, which are the time scale of spike emission.

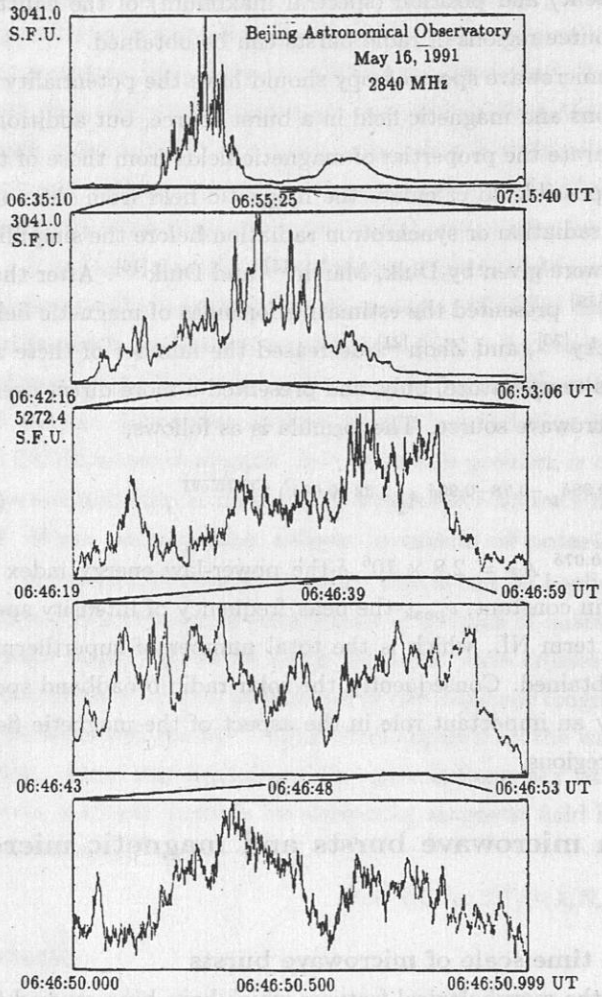

Fig.1 The time structures with different time scales in the event on May 16, 1991[22].

It is interesting that the fine temporal structures also appear in other wavebands, such as Hα (Fig.2[23]), Hard X-ray emission (Fig.3[24]), and so on. The remarkable fact is that although the burst time structures spread over a quite broad range, they are not randomly distributed. For individual bursts the scales of the temporal structures do not appear to form a continuum, rather they group into different ranges of scales. As a typical example, the event of May 16, 1991 is shown in Fig.1. It has been widely accepted that electrons accelerated or heated by flares in the solar corona are most directly detected from their gyromagnetic emission which is produced by means of interacting with magnetic field, and collisional bremsstrahlung with ambient plasma in the course of microwave bursts. The temporal structures of the emission of the microwave bursts reflect the production rate of the energetic electrons and the characteristic scales of the underlying kinetic instability. Consequently, the investigation on the time structures with different scales is essential to the study on flare physical processes, physical parameters of flare source regions, and in particular

the coronal magnetic fields.

3.2 Physical processes with different time scales

As mentioned above, the temporal structures with different time scales associate with the energy release processes in different speed. Kruger *et al.*[25] have discussed and compared some models for energy release with different time scales.

(1)Collisionless conduction fronts

The rise time of the microwave burst with the thermal flare mode, proposed by Brown *et al.*[26], and quantitatively analyzed by Batchelor *et al.*[27], is

$$\tau_r = l/c_s, \tag{7}$$

where l is the length of the loop, and c_s is the ion acoustic speed. For the parameters of average burst sources, $\tau_r \doteq 5$–55 s. This model has difficulties to explain regular structuring of subpulses and fine structures of emission at the ≤ 1 s scale.

(2) Twisted magnetic loop model

Sturrock *et al.*[28] proposed a nonthermal model, unwinding of a twisted "elementary flux tube" (EFT) as the elementary energy release process. The unwinding time is

$$\tau_u = l/V_A, \tag{8}$$

where V_A is the Alfvénic speed. The timescale is as high as 100 s, and this model probably acts too slowly.

(3) Coalescence model

Tajima *et al.*[29] proposed nonlinear current loop coalescence in a nonthermal model where the impulsive energy release again involves

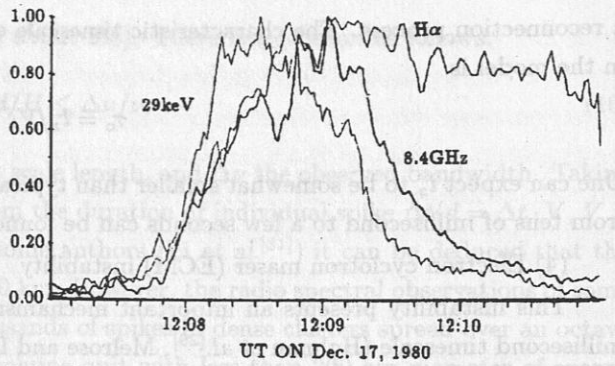

Fig.2 The comparison of the Hα lightcurve with the time profile of the corresponding event in the microwave region at 8.4GHz and in HXR at 29 keV clearly shows the close corresponding of some prominent spikes[23].

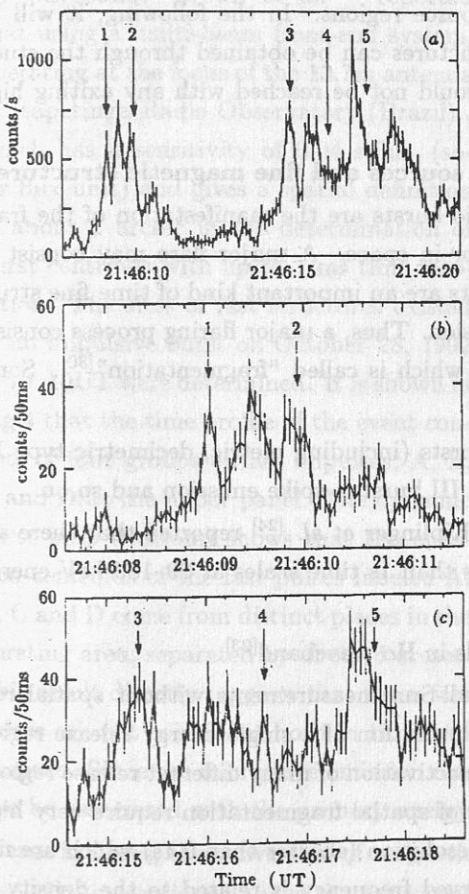

Fig.3 HXR time profiles (29–183 keV) at 50 ms per point of a solar flare which occurred on 1980 Oct. 18[24].

a reconnection process. The characteristic timescale of the duration of impulsive energy release in the model is

$$\tau_c = l_z / V_A \tag{9}$$

One can expect l_z to be somewhat smaller than typical loop lengths. The timescale of τ_c ranging from tens of millisecond to a few seconds can be found. It is a useful model.

(4) Electron cyclotron maser (ECM) instability

This instability presents an important mechanism for the production of the emission with millisecond timescale (Holman *et al.*[29], Melrose and Dulk[30], Sharma *et al.*[31]), where in flaring loops the maser emission at the electron–cyclotron frequency and its low harmonics strongly and rapidly produces by the energetic electrons with some special distribution. Due to the high growth rate, the timescale of the duration of impulsive energy release can be as short as 10^{-3}s, or less.

The mechanisms of energy release with different timescale mentioned above are closely related with magnetic field strength and configuration in source regions. In the following, it will be introduced that the information of fine magnetic structures can be obtained through the study of microwave FS. It is the diagnosing means which could not be reached with any exiting high spatial resolution radio instruments.

3.3 Spatial fragmentation of microwave burst sources and fine magnetic structures

The time structures with short timescale of radio bursts are the manifestation of the fragmentation of flaring processes in temporal domain or in space. A major flare may consist of thousands of type III bursts (microwave type III bursts are an important kind of time fine structures in microwave), and ten thousands of spike emission. Thus, a major flaring process consists of a great number of small energy release processes, which is called "fragmentation"[30]. Some examples are as follows.

(1) In the radio waveband, there are type III bursts (including metric, decimetric type III bursts, blips, type III-RS bursts, and microwave type III bursts), spike emission and so on.

(2) "Elementary flares" in the HXR waveband: Kiplinger *et al.* [24] reported that there are 53 out of 2830 HXR flares with rapid impulses of less than 1s time scales at 29–183 keV energy band (Fig.3).

(3) The sharp impulses with one to a few seconds in Hα waveband[23].

The above HXR and radio observations were full-Sun measurements without spatial resolution. They do not discriminate between the time evolution of a single energy release region accelerating electrons at a highly variable rate and the activation of many different release regions triggered by an initial disturbance. The observations of spatial fragmentation require very high spatial resolution (better than 0.″1) with high time resolution (shorter than 0.1s) which are not yet available. For coherent radio emission, the observed frequency is related to the density of the source (plasma emission) or its magnetic field (gyrofrequency) . Thus spatial resolution can be achieved by frequency resolution and time resolution, e.g. in a spectrogram. High resolution spectrograms have shown that the millisecond radio spike has extremely narrowband (0.4%–4%

of the center frequency with an average of about 2%). There is a relation as follows.

$$d/H \leq \Delta\nu/\nu, \tag{10}$$

where d is source diameter, H the relevant scale length, and $\Delta\nu$ the observed bandwidth. Taking $H = 10^4$km, then $d \leq 200$km. Besides, from the duration of individual spike $\Delta t (d = \Delta t \cdot V$, V is the disturbance speed) and argument of some authors (Li *et al.*[31]) it can be deduced that the source diameters are from a few tens to 200 km. However, the radio spectral observations of some major events have shown that tens of thousands of spikes in dense clusters spread over an octave in frequency. It means that these small volume unit with less than 200 km diameter of energy release regions must spread over a broad range. It is the phenomena of spatial fragmentation of burst sources. The other evidence of spatial fragmentation is as follows.

(1) Observational evidence in millimeter waveband: Brown *et al.*[32] reported that using a multi-beam front-end system, operating at the focus of the 13.7m antenna at Itapetinga Radio Observatory (Brazil) , which has a sensitivity of 0.04 s.f.u. (solar flux unit) and gives a spatial definition of about 2 arcsec in the determination of burst centroids with up to 1 ms time resolution. The sites of fast structures existed in an impulsive burst on October 28, 1992 at 10 :10UT were determined. It is shown in Fig.4 that the time profile of the event consists of four groups of fast impulses, A, B, C and D at the upper panel. The dynamic burst map (bottom) shows that the emission centroids of the fast pulses labeled A, B, C and D come from distinct places in the bursting area, separated by about 5 arcsec. This result directly suggests that these fast pulses are not coincident both in time and in space. Since the microwave emission can also be associated with the primary energy release in flares, the conversion of magnetic free energy is also "fragmentation".

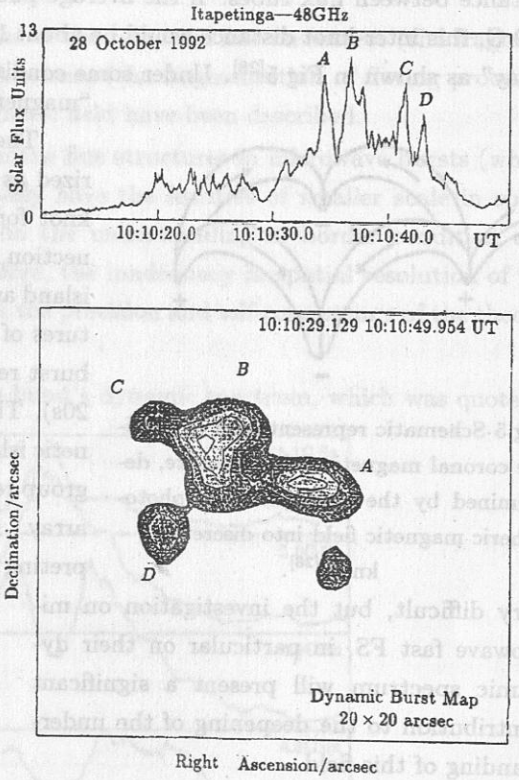

Fig.4 Upper: high speed pulsations from a millimeteric (48GHz) radio burst. Bottom: location of emission centroids for pulses A–D in the upper panel[32].

(2) As mentioned above the microwave emission in flares produces from that energetic electrons interacting with magnetic fields, so the fragmentation in space of microwave bursts may be attributed to the fragmentation of the magnetic structures, where exist relevant fine magnetic structures. Consequently, the finding of microwave fast FS is strong evidence of the "magnetic

elements". Sturrock *et al.*[28] proposed that the magnetic micro-structure patterns of "elementary-flux-tube" and "magnetic knot" are the relevant magnetic structures for the generation of energy release processes with very short timescale, and the magnetic field of active regions has a cell-like structure which could lead to a pulse-like structure in the time development of energy release. It was also pointed out that the variation of magnetic field from the smallest detectable values (a few gauss) to the values characteristic of sunspot umbrae (several thousand gauss) is not continuous. Observations[28] indicate that, at the photospheric level, magnetic field line tends to be pulled together into small flux regions with dimensions of an order of 500km or less, in which the magnetic field strength is of an order of 1000–1500 G. In consequence, the magnetic field at the photosphere tends to be aggregated into 'knot' in which the flux has values of order of $10^{18.4}$ Mx. The effect of the elementary-flux-tube structure would decay with height in a distance comparable with the distance between flux tubes. If the average photospheric field strength in an active region were 100 G, this inter-knot distance would be about 1500km, and they form the "elementary-flux-tube array" as shown in Fig.5[28]. Under some conditions, magnetic reconnection develops to form "magnetic islands" and "second islands".

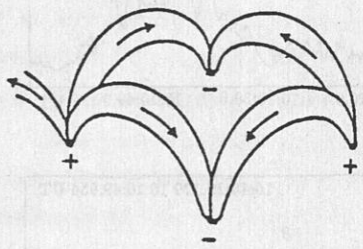

Fig.5 Schematic representation of possible coronal magnetic field structure, determined by the aggregation of photospheric magnetic field into discrete knots[28].

The basic concepts of this section can be summarized as follows . "Elementary-flux-tube" plus magnetic knot forms elementary flux tube array, and the reconnection among the elementary flux tubes forms magnetic island and secondary island. Thus we have the fine structures of the coronal magnetic field. An elementary flare burst represents energy release of a single flux tube (5–20s). The sub-bursts are due to the development of magnetic islands (tens to hundreds ms). An elementary burst group represents energy release of a elementary flux tube array. Certainly, these are assuming models for interpreting the fast bursts. The direct demonstration is very difficult, but the investigation on microwave fast FS, in particular on their dynamic spectrum will present a significant contribution to the deepening of the understanding of this field.

(3) Vlahos[32−34] proposed a working hypothesis of fine magnetic structures for the micro-energy release of producing "microflares" (microbursts). Subphotospheric and photospheric turbulence continuously splits the large scale magnetic tubes into millions of twisted flux tubes, which are isolated from each other. These are fibers and have different density and temperature profiles as a func-

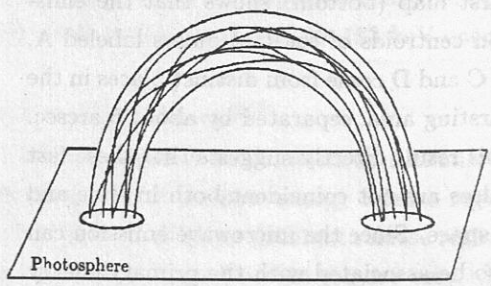

Fig.6 A large scale loop in composed of thousands of small scale fibers. Hundreds of thousands of small explosions form a "flare"[32].

tion of the distance from the photosphere, as shown in Fig.6. In the model described here the "flare" is the accumulation of N (thousands or millions) microflares that are triggered almost simultaneously. In this highly inhomogeneous environment reconnections, shock waves and MHD waves are simultaneously present. The energy release is fragmented. There are two levels of fragmentation: (i) fragmentation driven by the photosphere with the formation of fibres, (ii) local fragmentation due to the interplay of coalescence and tearing instability. MHD wave activity will be enhanced by the microflares and will drive new microflare activity. Their contribution is not simply the addition of N independent microflares, and the microflare is also not a scale down version of the flare. Many microflares acting together in a relatively small volume produce a different phenomenon which will be named "statistical flare". What is the cause of the sudden concentration of microflares in such a small volume? What is the cause that a large collection of small fibers suddenly to be triggered to reconnect?

From mentioned above, the internal relations of the temporal fine structures (the fragmentation of flares in time), fast processes of energy release (the fragmentation of flaring processes in space), and fine structures of the coronal magnetic field have been described.

The basic processes of plasma reflected from the fine structures in microwave bursts (where the magnetic fine structures deduced from) usually have the features of smaller scale in space and of variation in time, and do not depend on the understanding of border condition and parameter distribution in the large scale. Therefore, the inadequacy in spatial resolution of the radio observation will not produce an influence on the precision and self-consistency of the theory.

3.4 Some existing results in China

(1) Huang *et al.*[35,36] analyzed a microwave burst's dynamic spectrum, which was quoted

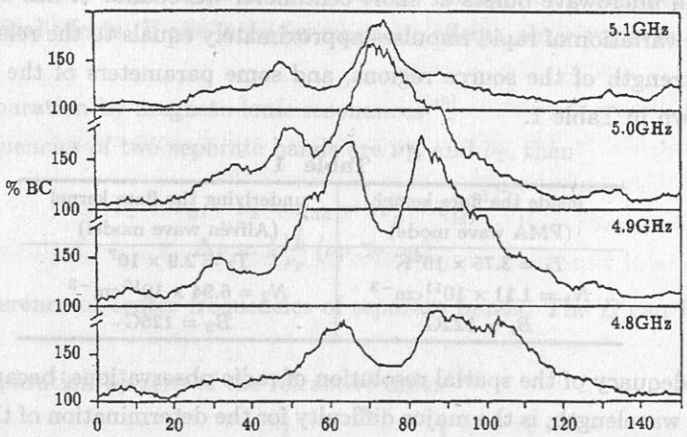

Fig.7 Flux density versus time profiles of some frequencies near the peak of an event of type "Hand" [37].

from observations of Allaart *et al.*[37] with 4–8GHz multichannels spectrometer at Dwingloo Radio Astronomical Observatory. This event with short time scale and narrow bandwidth was defined as type "hand" shown in Fig.7. The main characteristic of this event is that there are at least two pairs of positive and negative frequency drifts. The event is proposed as evidence of a magnetic

tube with a small scale and acceleration of electron beams with a short time scale at the source. From Fig.7, the frequency drift rate is $\pm 11\text{GHz}\cdot\text{s}^{-1}$, the relative bandwidth of this event is about 6%, and the time scale of single pulse is about 20–30 ms. Then, this FS has the mechanism similar to that of ms spikes in decimeter waveband, and the emission is also excited by some kind of plasma instability caused by nonthermal electrons. Thus the characteristic frequency of the FS corresponds to ambient magnetic field (electron gyrofrequency or its high harmonic at the sources), and the phenomenon of frequency drift reflects the existence of small scale inhomogeneity of the magnetic field along the direction of the nonthermal electron's movement. In Fig.7, the phenomenon which the frequency drift rates reverse from positive to negative or inversely, may directly interpret that the nonthermal electrons trapped in magnetic flux tubes with small scale are reflected back and forth, or the plasma instability is excited by that the nonthermal electrons cross through the sections of magnetic flux tubes. It is deduced from the observations and theoretical analysis that the average velocity of nonthermal electrons is about 0.1 c, the density of the electron beam is about $10^4\cdot\text{cm}^{-3}$ (10^{-4} of that of the ambient electrons), and the dimension of a micro-magnetic tube is about 600km, with information of various micro-magnetic structures.

Due to the corresponding relation between characteristic frequency and magnetic field strength of source regions, the scale of source region and one dimentional distribution of the magnetic field can be deduced from frequency drift, if the average speed of energetic electrons is known. Hence, a wealth of information containing in the dynamic spectra of the solar radio FS is very important for understanding the mechanism of solar flares, the parameters of source regions, and in particular the magnetic fields. The paper[35] is a good example.

(2) Li, and Qin[38] proposed a "dual quasi-periodic pulsation model" for interpreting the fast FS superposed on microwave bursts at short centimeter waveband. It has been proved that the relative intensity variation of rapid impulses approximately equals to the relative variation of the magnetic field strength of the source regions, and some parameters of the source regions were obtained, as shown in Table 1.

Table 1

inside the flare kemel (FMA wave mode)	underlying the flare kernel (Alfvén wave model)
$T_1 = 3.75\times10^6\text{K}$	$T_2 = 2.9\times10^7$
$N_1 = 1.11\times10^{11}\text{cm}^{-3}$	$N_2 = 6.94\times10^{10}\text{cm}^{-3}$
$B_1 = 122\text{G}$	$B_2 = 126\text{G}$

(3) The inadequacy of the spatial resolution of radio observations, because of the overlength of the long radio wavelength, is the major difficulty for the determination of the spatial position of the sources of microwave ms bursts, but it may be mitigated by making comprehensive analysis using the data both in radio and optical wavebands. The work of Fu *et al.*[39] is a tentative attempt of this kind of analysis. Some very well data of the October 2, 1993 event[40], including time profiles at three frequencies of 10 cm waveband and two dimension spectrogram and video record in Hα waveband were obtained. The results show that there are considerable correlation[41] between the two wavebands, and both the complicated impules group and microwave type III

burst group can be found in a small region of $2'' \times 2''$ arcsec, and that suggests a spatial fine magnetic field configuration. A paper of the results is in preparation.

4 Some radio spectral phenomena and the coronal magnetic field

Since the emission of quiet Sun and S-component at meter wave is rather weak, magnetic field estimation is mostly taken from the imformation on radio bursts.

4.1, MHD shock wave and slow-drift bursts[2]

The type II bursts' frequency drift rate depending on the shock velocity and the phenomenon of band splitting in type II bursts have been used for a long time to derive information about magnetic fields. Difficulties arise from the fact that a uniform and generally accepted theory of type II bursts is still missing.

(1) Shock velocity

There are different approaches to explain how plasma waves are excited by shock waves associated with type II bursts. According to the earliest approach by Pikelner and Gintsburg[42], the Langmuir waves are excited by a MHD shock if the Alfvénic Mach number M_A exceeds a critical Mach number M_c given by

$$M_A = \frac{v}{v_A} > M_c = 1 + \frac{3}{8}\left(\frac{8\pi NkT}{B^2}\right), \tag{11}$$

where $\frac{B^2}{8\pi} \gg NkT$ and $\nu_B \ll \nu_p$, and ν_p is plasma frequency. The B can be deduced from (11).

(2) Band splitting

The effect of band splitting of type II bursts can be interpreted in different ways either by magnetic or geometrical effects. If one looks for magnetic effects, three variants of interpretation are to be noted:

(i) Emission separation by magneto-ionic resonances[43]

The center frequencies of two separate bands are ν_1, and ν_2, then

$$\begin{gathered} \nu_1 = \nu_p, \quad \nu_2 = \nu_{uh} = \left(\nu_p^2 + \nu_B^2\right)^{1/2}, \\ \Delta\nu \approx \tfrac{1}{2}\tfrac{\nu_B^2}{\nu_p} \left(\nu_P \gg \nu_B\right), \end{gathered} \tag{12}$$

where $\Delta\nu$ is the difference of center frequencies of separate bands. The B can be deduced from ν_B.

(ii) Emission separation by zero of the refractive index[44]

$$\nu_1 = \nu_p; \quad \nu_2 = \nu_p + \frac{1}{2}\nu_B; \quad \Delta\nu = \frac{1}{2}\nu_B (\nu_p \gg \nu_B) \tag{13}$$

(iii) Another approach was proposed by Serd, Sheridan and Stewart[45] by deriving the related Mach M number from the Rankine-Hugoniot jump condition and hence again concluding the magnetic field from the shock speed is obtained.

$$B = 5.1 \times 10^{-5} v[\mathrm{km \cdot s^{-1}}] \nu_p[\mathrm{MHz}] M^{-1}[\mathrm{G}], \tag{14}$$

where v is shock speed, and ν_p is plasma frequency ahead the shock front.

4.2 Fast drift bursts[2]

(1) Polarization of harmonic radiation

According to Melrose *et al.*[46] the degree of polarization P of the second harmonic of the plasma frequency is

$$P = f(\theta, \theta_0)\frac{\nu_P}{\nu_B}, \tag{15}$$

where f is a function of the angle θ between wave propagation and the magnetic field B, and θ_0 denotes the limiting cone angle of the distribution of Langmuir waves.

(2) Time profile of ordinary polarization

Due to propagation, the time profile of the degree of polarization of a fast drift burst indicates the magnetic field. At the beginning of such bursts the totally polarized part corresponds to the distance Δs between the escape level of the ordinary and extraordinary wave modes so that

$$\Delta s = v_d \Delta t = \frac{\nu_B}{\nu} L_N, \tag{16}$$

where v_d is the drift velocity of the exciter and

$$L_N = N_e \left[\frac{dN_e}{ds}\right]^{-1}$$

is the scale height of the electron density N_e[47].

4.3 Spectral fine structures[2]

Spectral fine structures are abundant in nearly all types of solar meter wave emission. Technical difficulties of the magnetic field determination often arise from the lack of simultaneous spectral and spatial resolution. Examples of basic processes coming into consideration for magnetic field diagnostics are in the following.

(1) Double plasma resonance

The condition for double plasma resonance $\nu_p = S\nu_B$ was applied to the interpretation of fine structures in U-type bursts and Zebra patterns[48,49].

(2) Whistler waves

The drift rate of fiber bursts interpreted as signature of whistler waves is given by

$$D = \frac{d\nu}{dt} = \frac{\nu}{L_B} v_w = 2c\left(\frac{\nu_B}{\nu_p}\right)\left(\frac{\nu_W}{\nu_B}\left(1 - \frac{\nu_W}{\nu_B}\right)^3\right)^{1/2}, \tag{17}$$

where v_W is the group velocity and ν_W the frequency of whistler wave, respectively [50].

The possibility of calculating the magnetic field by means of the fine structures in microwave burst spectrogram and some results will be introduced in the last section.

4.4 Radio pulsation in coronal loops

The pulsation in radio bursts is a kind of fine structure of radio bursts which frequently appear and contain a wealth of useful information of source regions, and using these information some physical parameters and the magnetic field and magnetic structures of source regions can

be deduced. The radio telescopes and radio spectrometers with high time resolution are very powerful means for the investigation on radio pulsation. The pulsation period P is one of the parameters characterizing pulsating structure. Observed periods are usually assumed to be in the range of $0.5\text{s} < P < 50\text{s}$, but periods have also been observed as short as tens ms and amounting to 2–5 min, and the most common are 0.5–5 s. Aschwanden[51] presented an extensive review of the radio quasi-period pulsation in coronal loops. The radio pulsation are classified in three groups according to their driver mechanisms:

(1) Magnetic flux tube oscillations (the emissivity of trapped particles is modulated by a standing or propagating MHD wave).

(2) Cyclic self-organizing system of plasma instability (wave-particle, wave-wave inter-actions), and

(3) Modulation of acceleration (acceleration/injection of particles into the source).

Now, we only briefly introduce the MHD oscillations which have been more frequently studied and applied. The theoretical aspect of this model can be found in Roberts *et al.*[52] For the magnetoacoustic oscillations in compact magnetic flux tube, the characteristic time is [52]

$$P = 4a/v_{\mathrm{A}}, \tag{18}$$

where a is the radius of the tube and v_{A} is the Alfvén velocity. Taking $P = 0.1$ s, $a = 100$ km (the dimensions of fast burst source are tens–200 km), then, $\nu_{\mathrm{A}} = 4 \times 10^3 \mathrm{km} \cdot \mathrm{s}^{-1}$, and the magnetic field can be estimated. In the case of reflections in a trap, one has the length of the trap,

$$l = P \cdot v \tag{19}$$

where v is the velocity of the fast particle. Assuming $P = 0.05$ s, and $v = 10^5 \mathrm{km} \cdot \mathrm{s}^{-1}$, then the length of the magnetic flux tube is $l = 5000$ km. For propagating MHD wave[51],

$$P \approx 2.6\,(a/v_{\mathrm{A}})\,. \tag{20}$$

Thus it can be seen that the phenomenon of radio pulsations is also an important clue for the diagnosis of the coronal magnetic fields.

5 Summary and conclusions

5.1 Some existing results

Kruger and Hildebrandt[2] made a summary of the existing results of the raido measurement of the coronal magnetic fields, as shown in Fig.8. From [4], we have the average height distribution of coronal magnetic fields: a magnetic dipole field can be used as a reference model from which if the maximum field at photosphere is B_{m},the magneticfield at a height z above a sunspot can be deduced by

$$B_z = B_{\mathrm{m}} Z_{\mathrm{d}}^3 (Z + Z_{\mathrm{d}}^{-3}), \tag{21}$$

where Z_d is the fictive dipole depth below the photosphere. An analysis of 36 compact S-component sources observed at RATAN-600 is consistent with an average magnetic field at the bottom of the corona ($Z \approx 2 \times 10^3$ km) of 1750 G, with a magnetic scale height $L_B = B(Z)\,(\mathrm{d}B/\mathrm{d}Z)^{-1}$ of 7×10^3 km, and a gradient of the magnetic field $\mathrm{d}B_z/\mathrm{d}Z = (0.25 \pm 0.1)\mathrm{G} \cdot \mathrm{km}^{-1}$, corresponding to a gradient of $0.37\mathrm{G} \cdot \mathrm{km}^{-1}$ at the level of the photosphere. Same evidence of fields of 1800G existing in the corona above sunspots has been obtained by VLA observations (White *et al.*[55]). The force-free extrapolated photospheric field (black dots in Fig. 8) of a magnetogram measured on 4 July 1973 (Hildebrandt[56]) shows an astonishing agreement with the dipole distribution. Up to a height of about 1.5×10^5 km above the photosphere also the same dipole distribution is in accordance with fields derived from the reversal of circular polarization in QT-regions marked in by cross in Fig. 8 (Peterova and Ryabov[57]). In some contrast to the data quoted above, the magnetic fields derived from different burst observations can be different and partly exceed the maximum dipole field deduced from S-component observations. This is the case in particular for the fields obtained from the interpretation of fiber bursts by whistler wave[50] or from type II bursts[47]. Due to possible density irregularities, also for other magnetic field estimations the absolute height scale is not very certain[58,59], but it can be partly overcome

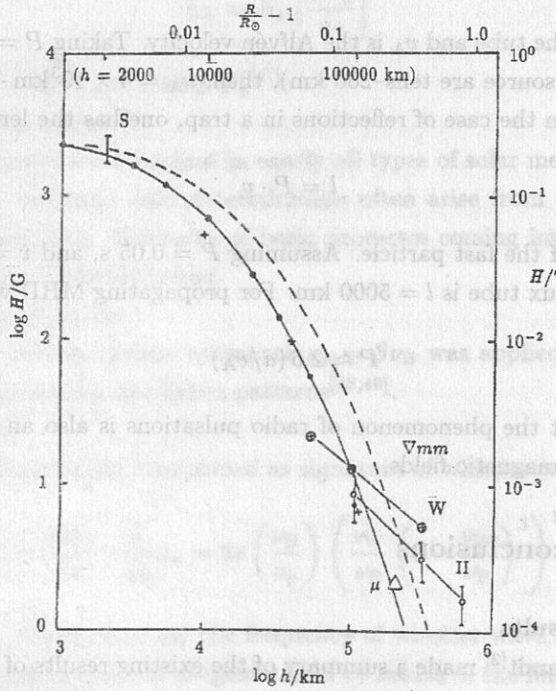

Fig.8 Measure of magnetic fields compared with dipole distribution above the center of a large sunspot ($B_m = 2500$ G, full line: dipole depth $Z_d = 2 \times 10^4$ km, broken line: $Z_d = 3 \times 10^4$ km); black dots refer to a force–free extrapolated photospheric field; s–s component, w–fiber bursts (whistler wave), II–type II bursts, M–microwave bursts (16.02.1984[53]), mm-mm bursts (29.09.1989[54])[2].

by limb observations. In a case, of an off-limb source provided the behind -limb flare on 16 February 1984[53], 8 GHz emission was detected at a height of $\geq 2\times10^5$ km above the photosphere (Fig.8). For the first time, 87 GHz radiation was recorded at presumably more than 3×10^5 km above the limb during the event on 29 September 1989[54]. In Summary, according to the present state of magnetic field estimated by radio methods, the following conclusions can be obtained[2]:

(1) Magnetic fields at the bottom of the corona up to about 2000 G are indicated by gyromagnetic radiation of the S-component. This is consistent with a dipole active region (sunspot) reference field with scale length of the order of 10^4 km in the low corona under nonflaring conditions.

(2) Magnetic field derived by various radio burst emissions tends to exceed the dipole distribution where direct height estimates from off -limb sources are in consistency with that obtained from indirect methods depending on given electron density models. Magnetic field transport by plasma flows may be responsible for a height dependence slower than $B \sim \mathrm{R}^{-3}$.

(3) Superimposed on the mean height distribution of magnetic fields, there is evidence for the existence of fine structures of the field for both flaring and nonflaring conditions.

(4) Magnetic fine structures are expected to be intimately related to fragmentary field dissipation (reconnection) leading to particle acceleration and plasma heating signified by radio emission.

5.2 A key research project of solar radio astronomy in China in the 23rd solar active cycle.

Now the radio approach of magnetic fine structures in solar atmosphere has been introduced. Because the radio method provides us with a unique quantitative measurement of the coronal magnetic field, considering the development of solar physics, solar activity and solar magnetic research which is the superiority in solar research in China, we should pay close attention to the study of the radio coronal magnetic fields and fine magnetic structures with radio methods. It should be taken as a key research project in the coming solar activity period.

Although the measurement of radio coronal magnetic fields in nonflaring time needs the equipment with high resolution in frequency and space which will not be established in China in the near future as mentioned above, the measurement of radio coronal magnetic fields in flaring time can be made using the equipment without spatial resolution, in particular the observation of microwave dynamic spectrogram with high time resolution, which provides us with a powerful means for the diagnosis of fine structure of the coronal magnetic fields. It is also the major scientific objects of the "Solar Radio Broadband Spectrometer" which is being set up as a key project for the 23rd solar active maximum period in China. The frequency range covered by this equipment is 0.7–8 GHz, corresponding to the regions of the height $5 \times 10^3 - 2 \times 10^5$ km (fundamental wave) and the range of electron density 10^{11}–$10^9 \mathrm{cm}^{-3}$ in solar atmosphere.

It should be emphatically pointed out that the solar magnetic field and its relation with solar activity are the important tasks in solar physics. Besides, solar radio astronomy is only one field of the research in solar physics, and therefore joint investigation of observation and theory

in radio, optical, UV and X-ray wavebands is required for final approach.

This work was supported by the grants of NSF of China and Chinese Academy of Sciences.

References

[1] Dulk G A. In: Mclean D J, Labrum N R eds. Solar radio physics. Cambridge: Cambridge Univ. Press, 1985. chap. 2

[2] Krüger A, Hildebrandt J. In: Zirin H, Ai G X, Wang H M eds. The magnetic and velocity fields of solar active regions, ASP Conf. Ser. Vol. 46, Proc. of IAU colloquium No.141, Beijing 1992, San Francisco: ASP 1993: 249

[3] Gelfreikh G B. Adv. Space Res. 1991, 11(1): 89

[4] Gelfreikh G B, Bogod V M. Abramov-Maximov V E *et al.* In: Zirin H, Ai G X, Wang H M. eds. The magnetic and velocity fields of solar active regions, APS Conf. Ser. Vol.46, Proc. IAU colloquium No.141, Beijing, 1992, San Francisco: ASP, 1993: 271

[5] Lang K R, Wilson J N, Kile J N *et al.* Ap. J., 1993, 419: 398

[6] Lee J W, Gary D E, Hurford G J. Solar Phys., 1993, 144: 45

[7] Kundu M R, Vlahos L. Space Sci. Rev., 1982, 32: 405

[8] Bogod V M, Gelfreikh G B. Solar Phys., 1980, 67: 29

[9] Gelfreikh G B, Lubyshev B I. Astron. Zh., 1979, 56: 562

[10] Alissandrakis C E, Kundu M R, Lantos P. Ap. J., 1980, 82: 30

[11] Krüger A, Hildebrandt J, Fürstenberg F. Astron. Astrophys., 1985,143: 72

[12] Holman G D, Kundu M R. Ap. J., 1985, 292: 291

[13] Zheleznyakov V V. Radio emission of the Sun and planets. New York: Pergamon Press, 1970

[14] Gelfreikh G B, Peterova N G, Ryabov B I., Solar Phys., 1987, 108: 89

[15] Dulk G A, Marsh K A. Ap. J., 1982, 259: 350

[16] Dulk G A. Ann. Rev. Astron. Astrophys., 1985, 23: 169

[17] Tandberg-Hanssen E, Emslie G A. The physics of solar flares. Cambridge: Cambridge Univ. Press, 1988

[18] Bastian T S, Gary D E. Solar Phys,. 1992, 139: 357

[19] Lim J, White S M, Kundu M R *et al.* Solar Phys., 1992, 140: 343

[20] Zhou A H, Karlicky M. Solar Phys., 1994, 153: 441

[21] Zhou A H. Astrophys. Space Sci., 1994, 222: 107

[22] Fu Qijun. In: Wang J X, Ai G X, Sakurai T *et al* eds. Proc. of the Third China-Japan seminar on solar physics, Dunhuang, China, 1994, Beijing: International Academic Publishers, 1995: 108

[23] Wülser J P, Kampfer N. NASA CP-2449, 1987, 301

[24] Kiplinger A L, Dennis B R, Emslie A G *et al.* Ap. J., 1983, 265: L99

[25] Krüger A, Kliem B, Hildebrandt J. Ap. J. Suppl. Ser., 1994, 90: 683

[26] Brown J C, Melrose D B, Spicer D S. Ap. J., 1979, 228: 592

[27] Batchelor D A, Crannell C J, Wiehl H J *et al.* Ap. J., 1985, 295: 258

[28] Sturrock P A, Kaufmann P, Moore R L *et al.* Solar Phys., 1984, 94: 341

[29] Tajima T, Sakai J, Nakajima T *et al.* Ap. J., 1987, 321: 1031

[30] Benz A O. Space Sci. Rev., 1994, 68: 135

[31] Li Chunsheng, Wang Deyu, Qin Zhihai. Acta Astronomica Sinica, 1988, 29: 69

[32] Vlahos L. In: Schmieder B, Priest E. eds. Dynamics of solar flares , Flares 22 workshop, Chantilly, France. 1990, Paris: Observatoire de Paris, DASOP, 1991: 91

[33] Vlahos L. Space Sci. Rev., 1994, 68: 39

[34] Vlahos, L. In: Benz A, Krüger A eds. Lecture Notes in Physics: Coronal magnetic energy releases, Proc. of the CESRA Workshop, Caputh/Potsdam, 1994, Berlin: Springer Verlag, 1995: 115

[35] Huang Guangli, Ni Jianping, Wang Rinyin. Acta Astrophysics Sinica, 1994, 14: 80

[36] Huang G L. In: Zirin H, Ai G X, Wang H M eds. The magnetic and velocity fields of solar active regions, ASP Conf. Ser. Vol .46, Proc. IAU Colloquium No.141, Beijing, 1992, San Francisco: APS, 1993: 279.
[37] Allaart M A F, Van Nieuwkoop J, Slottje C *et al.* Solar Phys., 1990, 130: 183
[38] Li Chunsheng, Qin Zhihai. Acta Astrophysica Sinica, 1993, 13: 174
[39] Fu Qijun, Li Chunsheng, Gong Yuanfang *et al.*, Solar Phys. 1993, 143, 317
[40] Fu Qijun, Qin Zhihai, Liu Yuying. In: Wang J X, Ai G X, Sakurai T *et al* eds. Proc. of the third China-Japan seminar on solar physics, Dunhuang, China, 1994, Beijing: International Academic Publishers, 1995: 157
[41] Huang Youran, Fang Cheng, Fu Qijun *et al.* Acta Astronomia Sinica, 1997, 38: 14
[42] Pikelner S B, Gintsburg M A. Astron, Zh. 1963, 40: 842
[43] Sturrock P A. Nature 1961, 192: 58
[44] Roberts J A. Aust. J. Phys., 1959, 12: 327
[45] Smerd S F, Sheridan K V, Stewart R T. Astrophys. Lett., 1975, 16: 22
[46] Melrose D B, Dulk G A, Smerd S P. Astron. Astrophys., 1978, 66: 315
[47] Fomichev V V, Chertok I M. Astron. Zh., 1965, 42: 1256
[48] Zheleznyakov V V, Zlotnik E Ya. Solar Phys., 1975, 44: 461
[49] Kuijpers J. Solar Phys., 1975, 44: 173
[50] Mann G, Baumgartl K, ESA SP-285, 1988: 153
[51] Aschwanden M J. Solar Phys., 1987, 111: 113
[52] Roberts B, Edwin P M, Benz A O. Ap. J., 1984, 279: 857
[53] Kruger A, Hildebrandt J, Kliem B *et al.* Solar Phys., 1991, 134: 171
[54] Kruger A, Urpo S, In: Svestka Z, Jackson B V, Machado M E eds. Lecture notes in physics: Eruptive solar flares. Berlin: Springer Verlag, 1992: 214
[55] White S M, Kundu M R, Gopalswamy N. Ap. J., 1991, 366: L43
[56] Hildebrandt J, Seehafer N, Kruger A. Astron. Astrophys., 1984, 134: 185
[57] Peterova N G, Ryabov B I. Astron. Zh., 1981, 58: 1070
[58] Bruggmann G, Benz A O, Magun A *et al.* Astron. Astrophys., 1990, 240: 506
[59] Lang K R, Wilson R F, Smith K L *et al.* Ap. J., 322: 1044